New Rhodium Complexes Coordinated by Bidentate Imine Ligands with Benzothiazolyl Functionalities

by **Gerrit R. Julius**, **Stephanie Cronje**, **Arno Neveling**, **Catharine Esterhuysen**, and **Helgard G. Raubenheimer***

Department of Chemistry, University of Stellenbosch, Private Bag X1, Matieland 7602, Stellenbosch, South Africa
(e-mail: hgr@sun.ac.za; tel: +27218083850; fax: +27218083849)

Dedicated to Professor *Dieter Seebach* on the occasion of his 65th birthday

The pseudo-square-planar complexes [Rh(cod)(Hbbtm)]BF_4 (**3**), [Rh(bbte)(cod)]BF_4 (**4**), [Rh$(CO)_2$(Hbbtm)]BF_4 (**5**), [Rh(bbte)$(CO)_2$]BF_4 (**6**), [Rh(bbtm)(cod)] (**7**) and [Rh(bbtm)$(CO)_2$] (**8**) (Hbbtm = bis(benzothiazol-2-yl)methane = 2,2′-methylenebis[benzothiazole], bbte = bis(benzothiazol-2-yl)ethane = 2,2′-(ethane-1,2-diyl)bis[benzothiazole], and cod = cycloocta-1,5-diene) were synthesized and characterized. Diastereotopic protons were observed for the protons at the bridge in the ^{1}H-NMR of **3** and **5**. Twisting of the ethane-1,2-diyl bridge in **4** and **6** effects chemical equivalence of the CH_2 groups in solution. Unusually large downfield shifts occur on coordination of the deprotonated ligand Hbbtm as the negative charge is delocalized in **7** and **8**. The NMR signals of the cod ligand in **4** could be differentiated. The X-ray crystal structures of **3**, **4**, and **6** are reported.

Introduction. – Our interest in rhodium complexes that contain ligands similar to compounds in biological systems has been raised since the successful use of rhodium complexes with H_2O-soluble biopolymers (human-serum albumin) as ligands in the hydroformylation of olefins [1]. Several groups have described the synthesis, characterization, and application of rhodium(I) complexes containing five-membered heterocycles in homogeneous catalytic transformations [2–11].

[Rh$(CH_2$\{mBnzim\}$_2)(CO)_2$]BPh_4 and [Rh$(CH_2$\{mim\}$_2)(CO)_2$]BPh_4 (mBnzim = methylbenzimidazolyl and mim = methylimidazolyl) have been structurally characterized [2] and used in the intramolecular hydroamination of terminal and nonterminal alkynes [3] and the cyclization of acetylenic carboxylic acids and acetylenic alcohols to afford O-containing heterocycles [4]. The methylene-bridge protons undergo exchange in deuterated solvents once the ligand is coordinated to the metal center. Accordingly, deprotonation of Hbbom (bis(2-benzoxazol-2-yl)methane) and reaction with [Rh$Cl(CO)_2]_2$ yielded [Rh(bbom)$(CO)_2$], but this complex proved to be a weak catalyst precursor for the reduction of nitrobenzene to aniline [5].

Oro and co-workers [6] have described the synthesis and structural characterization of mononuclear and binuclear rhodium(I) complexes with the general formulae [\{Rh$Cl(CH_2(pz)_2)$(cod)\}$_2$], [Rh$(CH_2(pz)_2)$(cod)]ClO_4 and [Rh$(CH_2(pz)_2)(CO)_2$]ClO_4 ($CH_2(pz)_2$ = bis(pyrazolyl)methane). Hydroformylation of hex-1-ene and heptenes are catalysed by [$Rh_2(CO)_2$\{$P(OPh)_3$\}$_2(\mu$-pz$)_2$] [7] and [Rh\{$P(OPh)_3$\}$_2$(pz)]$_2$ [8] (pz = pyrazolato) under mild conditions. Evidence that binuclear [$Rh_2Cl_2(cod)_2(L)$] complexes that contain bidentate *NN′* and tridentate *NN′N* 1-(alkylamino)pyrazoles exist as ionic species was recently presented [10]. Substitution of a CO ligand in

$[Rh(\mu\text{-pz})(CO)_2]_2$ (pz = pyrazolato or 3,5-dimethylpyrazolato) with 3-(diphenylphosphino)benzoic acid yields dinuclear and mononuclear complexes. The dinuclear complexes are substantially more active than the monorhodium compounds in catalytic hydroformylations [11].

Remarkable activity and enantioselectivity in the hydrosilylation of ketones was achieved with the related compounds [Rh(cod){2-[4,5-dihydro-4-isopropyloxazol-2-yl)methyl]pyridine}]PF_6 and [Rh(cod)(2-[(4,5-dihydro-4,4-dimethyloxazol-2-yl)methyl]pyridine}]PF_6 [9] as catalyst precursors. The ^{1}H-NMR spectra of these compounds indicate that the six-membered chelate ring undergoes conformational flipping or inversion.

Bidentate benzothiazole (thiazole units are present in vitamin B_1) ligands have not been examined in the above studies. The most successful hydroformylation catalysts in recent studies contain bidentate phosphine ligands [12], and the discovery that the hydroformylation of propene is accelerated by the addition of N-containing compounds like amines, amino acids, heterocycles, and urea derivatives [13] influenced our decision to focus on the preparation and characterization of rhodium(I) complexes with bidentate imine-coordinating benzothiazolyl-containing ligands for future use in hydroformylation reactions.

In this paper, we report the synthesis of [Rh(cod)(Hbbtm)]BF_4 (**3**), [Rh(bbte)(cod)]BF_4 (**4**), [Rh$(CO)_2$(Hbbtm)]BF_4 (**5**), [Rh(bbte)$(CO)_2$]BF_4 (**6**), [Rh(bbtm)(cod)] (**7**), and [Rh(bbtm)$(CO)_2$] (**8**) (Hbbtm = bis(benzothiazolyl)methane = 2,2′-methylenebis[benzothiazole], bbte = bis(benzothiazolyl)ethane = 2,2′-(ethane-1,2-diyl)bis-[benzothiazole], and cod = cycloocta-1,5-diene). Complete characterization of these compounds revealed interesting new structural features but also striking differences to related compounds.

Results and Discussion. – The addition of a solution of $[RhCl(cod)]_2$ in acetone, after treatment with $AgBF_4$, to a solution of the bidentate ligands **1** or **2** yielded the ionic complexes **3** and **4**, respectively [14] (*Scheme 1*). Compounds **3** and **4** were converted to the carbonyl complexes **5** and **6** by bubbling CO gas through solutions thereof in CH_2Cl_2. The yellow products are soluble in polar solvents (CH_2Cl_2, acetone) and insoluble in nonpolar solvents (pentane, hexane) and Et_2O.

Deprotonation of **1** with BuLi in Et_2O and the subsequent addition of $[RhCl(cod)]_2$ afforded the neutral chelate **7**, which could readily be converted to its carbonyl derivative **8** (*Scheme 2*). These two orange products are soluble in CH_2Cl_2, Et_2O, hexane, and pentane.

Fragmentation involving the loss of the cod ligand or the sequential loss of the CO ligands was observed in the MS of all the cationic and neutral complexes mentioned thus far. Peaks in the IR spectra were assigned to the two IR-active vibrations a′(symmetrical) and a″(antisymmetrical) expected for the complexes **5**, **6**, and **8**, which have only one mirror plane and belong to the C_s point group. The CO vibrations in **5** and **6** have higher wavenumbers (15–20 cm^{-1}) than those in the previously mentioned benzimidazolyl compounds [2], indicating that less e^- density is donated by the aromatic S-containing five-membered heterocycles [15]. The delocalized negative charge generated after deprotonation of the bridge proton in ligand **1** becomes available for donation to Rh and causes a lowering of the $\tilde{\nu}$(CO) wavenumbers. These correspond to

Scheme 1[1])

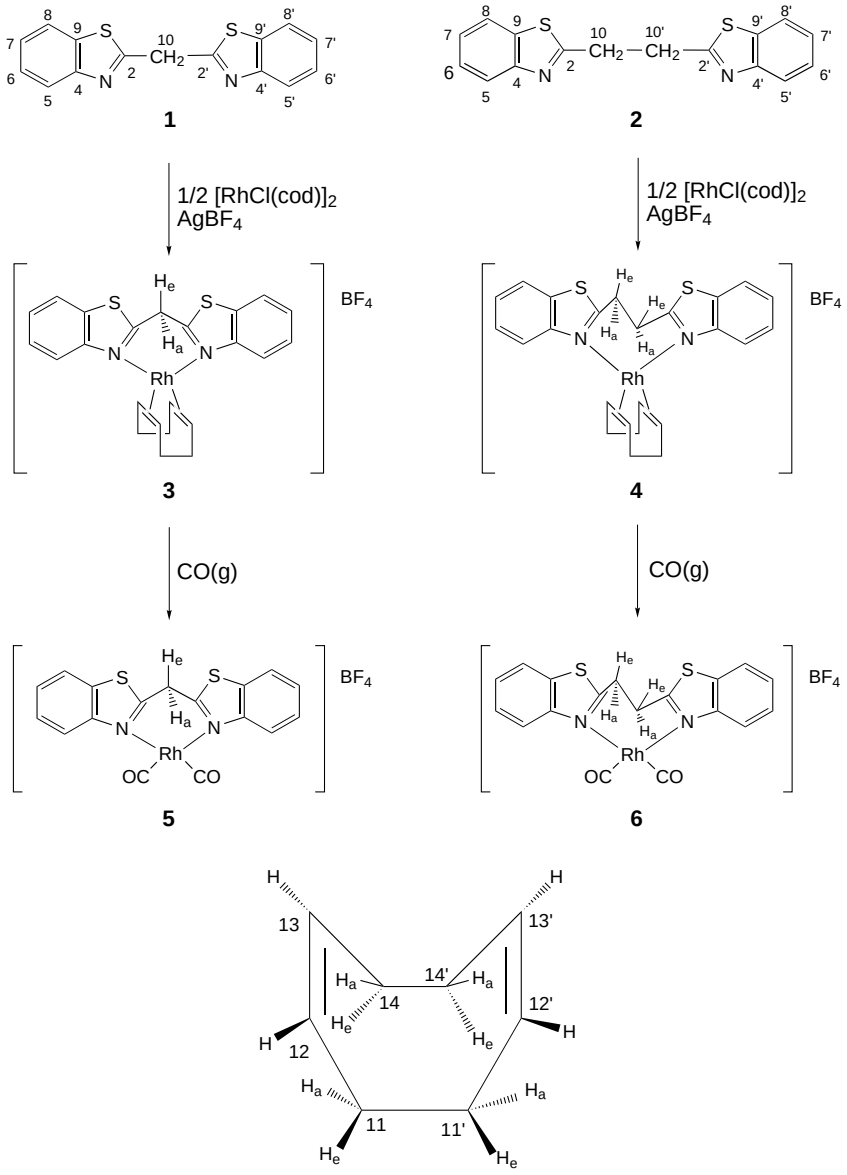

values observed for cationic imidazole complexes and a neutral benzoxazole complex [Rh(bbom)(CO)$_2$] (2069 and 2013 cm^{-1}) [5].

The NMR signals for the two benzothiazole rings in compounds **3**–**8** are equivalent. ^{1}H-NMR signals of the benzothiazole rings generally shift to a slightly lower field upon

[1]) The numbering of the ligands is arbitrary; see *Schemes 1* and *2* and *Figs. 1–3*.

Scheme 2[1])

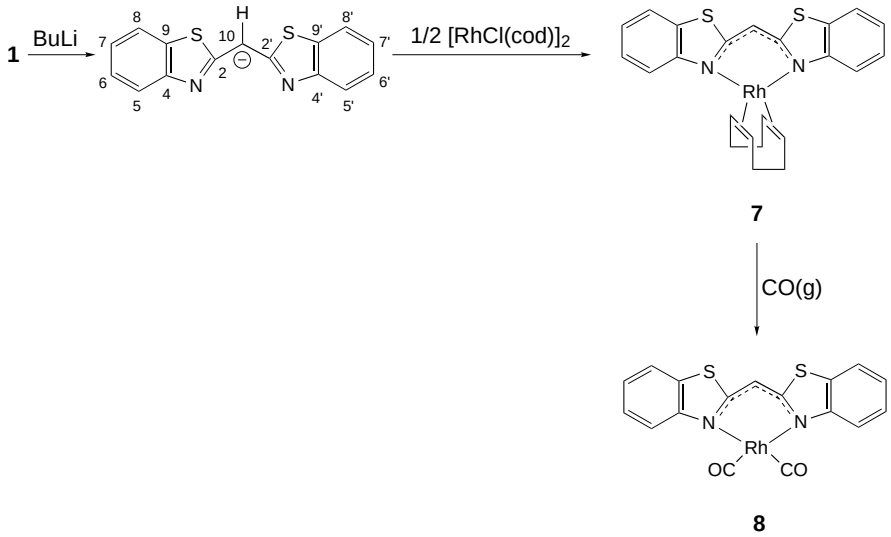

coordination, and slight upfield or downfield shifts in the δ values are observed in the ^{13}C-NMR spectra for compounds **3**–**6**. ^{13}C-NMR-Shift changes do not necessarily reflect local charge changes as the paramagnetic component of the chemical shift significantly contributes to the total chemical shift, unlike the chemical shift in ^{1}H-NMR spectra, which is totally determined by the diamagnetic contribution of the chemical shift and, thus, directly reflects local charge movement [16]. In compounds **7** and **8**, however, both the ^{1}H- and ^{13}C-NMR signals are shifted to a higher field upon coordination as a result of the additional delocalized negative charge after deprotonation.

The most distinctive feature of the ^{1}H-NMR spectra are the signals for diastereotopic protons (2 *d*, *AX* spin system) of the CH_2 bridge between the benzothiazole rings in the spectra of **3** (δ 5.57 and δ 6.03) and **5** (δ 5.66 and δ 5.29). The crystal-structure determination of **3** (*vide infra*) enabled us to assign the peaks unequivocally. The signals are shifted downfield from the signal of the free ligand (δ 4.95). The signal assigned to the equatorial proton (in the plane of the benzothiazole ring) has a larger chemical shift than the signal of the axial proton as it is deshielded by the magnetic anisotropic effect of the aromatic benzothiazole moiety. The coupling constants are similar to expected values for geminal protons (16–18 Hz) [17]. Conformational flipping or inversion of the six-membered chelate ring [9] rather than dimer formation [6] is probably responsible for the disappearance of diastereotopic protons at room temperature. A small angle ($<$) between the planes of the ligand rings that are bridged by the CH_2 ($< = 110.17^\circ$ in **3**) prevents conformational flipping or inversion and leads to the observation of the diastereotopic bridge protons. Thus no diastereotopic bridge protons have been reported for $[Rh(CH_2\{mBnzim\}_2)(CO)_2]BPh_4$ ($< = 136.95^\circ$) [2] or $[Rh(CH_2(pz)_2)(cod)]ClO_4$ ($< = 132.85^\circ$) [6], but they have been detected for $[Rh(CH_2(3,5\text{-}Mepz)_2)(cod)]ClO_4$ (δ 6.77, 7.80, $^{2}J = 15.6$ Hz; no structural

data) [6], [Rh(cod){2-[(4,5-dihydro-4-isopropyloxazol-2-yl)methyl]pyridine}]PF_6 (δ 4.9, 4.0, $^2J = 19$ Hz; $< = 113.95°$ and 124.70°) at room temperature and [Rh(cod){2-[(4,5-dihydro-4,4-dimethyloxazol-2-yl)methyl]pyridine}]PF_6 (δ 5.2, 4.3, $^2J = 15$ Hz; $< = 109.18°$) at $-90°$ [9].

The CH_2CH_2-bridge protons (δ 3.73 in the free ligand) of **4** (δ 4.18 and 5.40) and **6** (δ 4.10 and 4.70) are observed as two *m*. These protons are geminally and vicinally coupled to their neighbors resulting in a *m* (*AA′BB′* spin system). The crystal-structure determination of **4** (*vide infra*) shows deshielded equatorial protons in the same plane as the benzothiazole rings and axial protons perpendicular to this plane, and that the CH_2CH_2 protons and C-atoms are in chemically different environments in the solid state. Probably, as a result of twisting of the bridge in solution, which does not cause a disturbance of the mirror plane, only two and not four signals are observed for the protons, and one signal and not two signals are observed for the C-atoms.

An unusual downfield shift ($\Delta\delta$ 44.51 for Hbbtm and **8**) of the signal for the bridge C-atom to δ 85.14 in **7** and δ 83.84 in **8**, occurs upon deprotonation and coordination of Hbbtm. A similar shift, albeit smaller ($\Delta\delta$ 32.79), has been reported for the bis(benzoxazol-2-yl)methane ligand in [Rh(bbom)$(CO)_2$] [5]. It seems that the negative-charge delocalization in the S-containing rings is significantly better than in the oxazole rings.

The signals for four olefinic protons of the cod ligand in **3** are as expected. In the ^{1}H-NMR spectrum of **4**, two sets of broad *s* are observed for the four olefinic protons at δ 4.69, for H–C(12) and H–C(12′) (deshielded by the anisotropic effect of the pseudoaromatic benzothiazole rings) and at δ 4.48 for H–C(13) and H–C(13′)-facing the CH_2CH_2 bridge (less deshielded by the benzothiazole rings)[1]). Five signals for the cod ligand and no ^{13}C-NMR data have been reported for the cod ligand in [Rh(cod){2-[(4,5-dihydro-4-isopropyl)oxazol-2-yl)methyl]pyridine}]PF_6 [9]. The signals in the ^{13}C-NMR of **4** at δ 87.33 for C(12) and C(12′) and at δ 83.86 for C(13) and C(13′) are coupled to Rh and the coupling constants are 11.69 Hz. Similar Rh,C coupling constants have been described for the olefinic cod C-atoms in the ^{13}C-NMR spectra of [Rh(CH_2(pz)$_2$)(cod)]ClO_4 (δ 83.5, J(Rh,C) = 12.4 Hz) and [Rh(CH_2(3,5-Mepz)$_2$)(cod)]ClO_4 (δ 85.3, J(Rh,C) = 12.4 Hz) [6].

The aliphatic protons at the cod ligand of **3** are observed as *m* at δ 2.69 for the equatorial protons (in the same plane as the olefinic protons, deshielded by anisotropy of the C=C bond) and δ 2.05 for the axial protons (perpendicular to the olefinic protons, shielded by anisotropy of the C=C bond). One signal at δ 30.81 represents the aliphatic C-atoms in the ^{13}C-NMR of **3**. The benzothiazole-deshielded equatorial aliphatic protons of **4** appear as 2 *m* at δ 2.92 (H–C(11), H–C(11′)) and 2.74 (H–C(14), H–C(14′)) in the ^{1}H-NMR, and the aliphatic C-atoms at δ 31.03 and 30.80 in the ^{13}C-NMR. The aliphatic C-atoms in the ^{13}C-NMR of [Rh(CH_2(pz)$_2$)(cod)]ClO_4 and [Rh(CH_2(3,5-Mepz)$_2$)(cod)]ClO_4 have been reported at δ 31.0 and 31.2, respectively [6]. The axial protons are observed at δ 2.14. The *m* ascribed to the equatorial protons result from geminal coupling to the neighboring proton located at the same C-atom, vicinal coupling to the protons at the neighboring C-atom, and coupling to the olefinic protons as the dihedral angle approaches 0° and the coupling constant has a maximum value. The axial protons are geminally coupled to the neighboring proton located at the same C-atom and vicinally coupled to the protons at the neighboring C-atom but not, or minimally, to the olefinic proton as the dihedral angle approaches 90° and the coupling constant has a minimum value.

The ^{13}C-NMR signals for the carbonyl groups of **5**, **7**, and **8** are observed between δ 182 and 188 with coupling constants ranging between 67 and 71 Hz, well within the range of values observed for similar compounds, [Rh(CH_2{mim}$_2$)$(CO)_2$]BPh_4 (δ 186.0, J(Rh,C) = 67.6 Hz), [Rh(CH_2{mBnzim}$_2$)$(CO)_2$]BPh_4 (δ 189.8, J(Rh,C) = 68.1) [2] and [Rh(bbom)$(CO)_2$] (δ 185.53, J(Rh,C) = 67.6 Hz) [5].

The crystal structures of **3**, **4**, and **6** are shown in *Figs. 1–3*, and selected bond lengths and angles are shown in the *Table*. The Rh-atom is centered in an essentially square-planar arrangement defined by two N-atoms of the bidentate ligands and the centres (centroid C(123) and C(123′)) of the C=C bonds of the cod ligand in **3** and **4** or

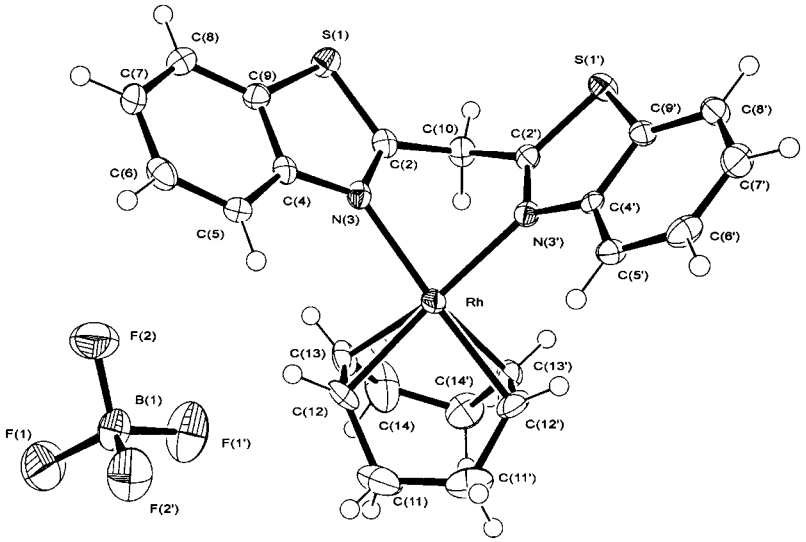

Fig. 1. *Molecular structure of complex* **3** *showing the numbering scheme.* Ellipsoids are shown at the 50% probability level.

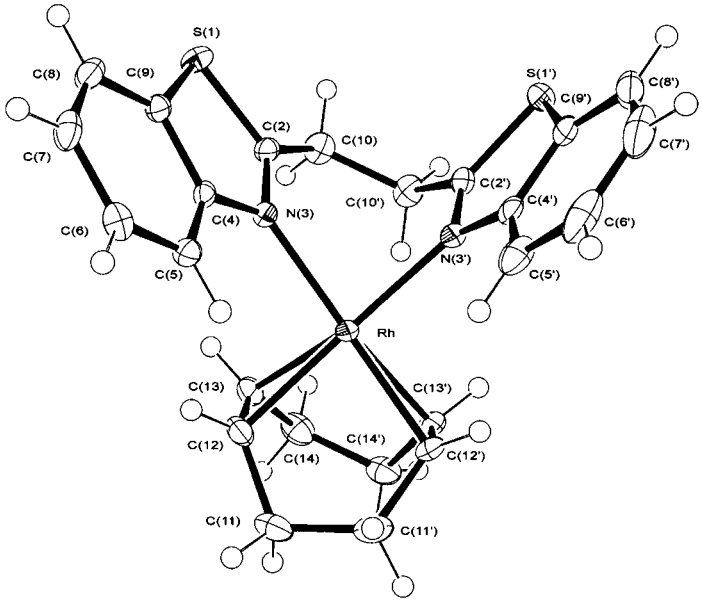

Fig. 2. *Molecular structure of the cation of complex* **4** *showing the numbering scheme.* Ellipsoids are shown at the 50% probability level. The solvent CH_2Cl_2 and the BF_4^- anion are omitted for clarity.

the CO ligands in **6**. The four olefinic C-atoms of the cod ligand in **3** and **4** have a maximum deviation from the plane formed by these C-atoms, the Rh-atom ($-0.181(1)$ Å for **3** and 0.098(1) Å for **4**), and the two N-atoms of the bidentate

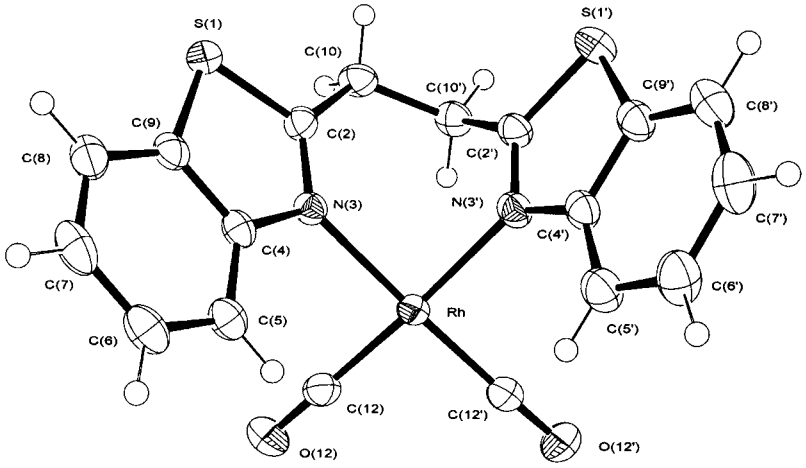

Fig. 3. *Molecular structure of the cation of complex* **6** *showing the numbering scheme.* Ellipsoids are shown at the 50% probability level. The solvent CH_2Cl_2 and the BF_4^- anion are omitted for clarity.

Table. *Selected Bond Lengths and Angles for Compounds* **3**, **4**, *and* **6**

	3	**4**	**6**
Bond lengths [Å]: Rh–N(3), Rh–N(3′)	2.137(2), 2.113(2)	2.0967(16), 2.1087(16)	2.108(2), 2.084(2)
Rh–C(12), Rh–C(12′)	2.149(3), 2.147(3)	2.163(2), 2.140(2)	1.869(3), 1.861(3)
Rh–C(13), Rh–C(13′)	2.137(3), 2.133(3)	2.136(2), 2.147(2)	
Rh–C(123), Rh–C(123′)	2.031(3)[a]), 2.026(3)[a])	2.033(2)[a]), 2.027(2)[a])	
C(12)–O(12), C(12′)–O(12′)			1.123(3), 1.123(3)
C(2)–C(10), C(2′)–C(10′)	1.499(4), 1.508(4)	1.505(3), 1.499(3)	1.496(4), 1.498(4)
C(10)–C(10′)		1.539(3)	1.534(4)
Bond angles [°]: N(3)–Rh–N(3′)	82.04(9)	82.67(6)	85.76(8)
C(12)–Rh–N(3)	101.31(11)	97.81(7)	91.95(10)
C(12′)–Rh–N(3′)	94.98(11)	95.13(7)	92.04(10)
C(13)–Rh–N(3)	88.24(11)	91.11(7)	
C(13′)–Rh–N(3′)	92.10(10)	93.12(7)	
C(123)–Rh–N(3)	95.03(11)[a])	94.73(8)[a])	
C(123′)–Rh–N(3′)	93.75(11)[a])	94.35(8)[a])	
C(123)–Rh–C(123′)	87.30(12)[a])	87.80(9)[a])	
C(12)–Rh–C(12′)			90.29(12)
Rh–N(3)–C(2)	112.71(19)	123.85(13)	127.23(17)
Rh–N(3′)–C(2′)	115.59(18)	115.68(14)	117.36(18)
N(3)–C(2)–C(10)	122.8(3)	127.18(18)	128.5(2)
N(3′)–C(2′)–C(10)	120.6(2)		
N(3′)–C(2′)–C(10′)		121.3(18)	121.4(2)
C(2)–C(10)–C(2′)	107.7(2)		
C(2)–C(10)–C(10′)		117.67(17)	117.2(2)
C(2′)–C(10′)–C(10)		114.51(18)	114.5(2)

[a]) C(123) and C(123′) are the centroids of C(12)–C(13) and C(12′)–C(13′), respectively. The standard deviations were calculated as the averages of the corresponding bond lengths and angles of the C-atoms in the cod ligand.

ligands (N(3) 0.066(2) Å and N(3′) −0.090(2) Å for **3**; N(3) 0.100(1) Å and N(3′) −0.086(1) Å for **4**). The two N-atoms of the ligand in **4** are slightly deviated on either side of the plane. This can be attributed to the orientation of the CH_2CH_2 bridge in the ligand. The Rh-atom, two N-atoms and two C-atoms of the CO ligands in compound **6** are coplanar (Rh −0.019(1) Å, N(3) −0.031(1) Å, N(3′) 0.039(1) Å, C(12) 0.043(1) Å, C(12′) −0.033(1) Å).

The bite angles of the Hbbtm and bbte ligands in **3** (N(3)−Rh−N(3′) 82.04°) and **4** (N(3)−Rh−N(3′) 82.67°) and the steric bulk of the cod ligands in **3** and **4** induce some deviation from the ideal 90° bond angles around the central Rh-atom. The bite angle of the bidentate ligand in **3** is smaller than the bite angle of the bis(pyrazolyl)methane ligand (N−Rh−N 88.4(3)°) in the complex $[Rh(CH_2(pz)_2)(cod)]ClO_4 \cdot 1/2\ C_2H_4Cl_2$ [6], but the Rh-olefinic centroid angles are the same. The longer bridge in the bbte ligand of **4** does not result in a much larger bite angle (N(3)−Rh−N(3′) 82.67°) but is rather accommodated by distortion of the bridge (N(3)−C(2)−C(10) 127.18°, N(3′)−C(2′)−C(10′) 121.3°, C(2)−C(10)−C(10′) 117.67° and C(2′)−C(10′)−C(10) 114.51° in **4** and N(3)−C(2)−C(10) 128.5°, N(3′)−C(2′)−C(10′) 121.4°, C(2)−C(10)−C(10′) 117.2° and C(2′)−C(10′)−C(10) 114.5° in **6**).

Substitution of the sterically demanding cod ligand with the smaller CO ligands in **6** results in a larger bite angle for the bbte ligand (N(3)−Rh−N(3′) 85.76°) and less deviation from the idealized 90° for the other ligands around the Rh-atom (C(12′)−Rh−C(12) 90.29°, C(12)−Rh−N(3) 91.95°, and C(12′)−Rh−N(3′) 92.04°).

The Rh−N distances are all similar and correspond to the separations in $[Rh(CH_2(pz)_2)(cod)]ClO_4 \cdot 1/2\ C_2H_4Cl_2$ [6] and $[Rh(CH_2(mBnzim)_2)(CO)_2]BPh_4$ [2]. The structure of the cod ligand in complex **3** is similar to that of **4**, $[Rh(CH_2(pz)_2)(cod)]ClO_4 \cdot 1/2\ C_2H_4Cl_2$ [6], and [Rh(Cl(1,3-dihydro-1,3-dimethyl-2*H*-imidazol-2-ylidene)(cod)] [18]. The Rh−CO bond lengths in **6** are comparable to those in $[Rh(CH_2\{mBnzim\}_2)(CO)_2]BPh_4$ [2]. Bond lengths and angles in the thiazole units of the ligands of **3**, **4**, and **6** are essentially the same and similar to those reported for thiazole units in $[(CO)_3\overline{FeS{=}C(SCH_3)C{=}NC_6H_4S}\text{-}o]$ [19] and $[\{C(HO)(C_6H_5)(\overline{C{=}NC_6H_4S}\text{-}o)_2\}ZnCl_2]$ [20].

The angle between the planes (<) of the benzothiazole rings decreases from 110.17° for **3** to 99.6° for **4** and 93.63° for **6** and is smaller than the same angle in similar compounds: $[Rh(CH_2\{mBnzim\}_2)(CO)_2]BPh_4 <= 136.95°$ [2], $[Rh(CH_2(pz)_2)(cod)]ClO_4 <= 132.85°$ [6], [Rh(cod){2-[(4,5-dihydro-4-isopropyloxazol-2-yl)methyl]pyridine)}]$PF_6 <= 113.95°$ and 124.7°, and [Rh(cod){2-[(4,5-dihydro-4,4-dimethyloxazol-2-yl)methyl]pyridine]}]$PF_6 <= 109.18°$ [9]. Accommodation of the longer bridge in the bbte ligand and the cod ligand in **4** also causes a larger angle between the plane of each of the benzothiazole units and the plane formed by the Rh- and N-atoms (73.13(6)° and 73.45(5)°) compared to the corresponding angles in **3** (61.17(7)° and 55.81(8)°, smaller CH_2 bridge) and **6** (62.22(5)° and 62.25(6)°, no restriction of bbte by sterically demanding cod ligand).

Conclusions. – Several interesting structural features of rhodium complexes containing bidentate imine ligands derived from thiazoles were illustrated. Smaller angles between the planes of the benzothiazole rings in the Hbbtm and bbte ligands prevent conformational flipping or inversion. Diastereotopic protons are observed in

the ^{1}H-NMR spectra of [Rh(cod)(Hbbtm)]BF_4 (**3**) and [Rh(CO)$_2$(Hbbtm)]BF_4 (**5**). Twisting of the CH_2CH_2 bridge in [Rh(bbte)(cod)]BF_4 (**4**) and [Rh(bbte)(CO)$_2$]BF_4 (**6**) in solution induces chemical equivalence of the CH_2 groups in the NMR spectra of these compounds. The bridge C-atoms in the ^{13}C-NMR spectra of [Rh(bbtm)(cod)] (**7**) and [Rh(bbtm)(CO)$_2$] (**8**) are shifted severely downfield as a result of delocalization of the negative charge. The signals of the cod ligand in the NMR spectra of **4** allow differentiation between two groups of olefinic C-atoms and protons, two groups of aliphatic C-atoms and protons, and an additional group of axial aliphatic protons. The IR spectra of **5** and **6** indicate that e^- density located in the pseudoaromatic benzothiazole-containing ligand is less available for donation to the Rh than in imidazole-containing ligands.

Experimental Part

General. All reactions and manipulations were performed under N_2 by standard vacuum-line and *Schlenk* techniques. All solvents were dried and purified by conventional methods and were freshly distilled under N_2 before use [21]. Other reagents were used as received from commercial suppliers. Butyllithium was standardized [22]. Hbbtm (**1**), bbte (**2**) [23], and [RhCl(cod)]$_2$ [24] were prepared according to literature procedures. M.p.: *Büchi-535* apparatus, in open capillaries; uncorrected. IR Spectra: *Perkin-Elmer 1600-FTIR* spectrometer; in cm^{-1}. NMR Spectra: *Varian Gemini-2000* spectrometer, ^{1}H at 299.65 MHz and ^{13}C{^{1}H} at 75.48 MHz; chemical shifts δ in ppm, reported relative to the solvent resonance, J in Hz. Mass Spectra: *VGA 70-70E* instrument, FAB at 70 eV with xenon as bombardment gas and 3-nitrobenzyl alcohol as matrix; in m/z (rel. %). Elemental analyses: *Fisons CHNS-1108* elemental analyser.

[Rh(cod)(Hbbtm)]BF_4 (**3**). A soln. of [RhCl(cod)]$_2$ (0.111 g, 0.225 mmol) in acetone (20 ml) was treated with $AgBF_4$ (0.088 g, 0.452 mmol) at r.t., and the mixture was stirred for 30 min. AgCl formed as a precipitate. The mixture was filtered into a *Schlenk* tube containing a solution of Hbbtm (0.127 g, 0.450 mmol) in acetone (20 ml). The color of the mixture changed from yellow to orange, and the acetone volume was reduced to 1–2 ml *in vacuo*. Compound **3** was precipitated by the addition of Et_2O (15 ml). The yellow precipitate (0.245 g, 94%) was filtered and washed with Et_2O (2 × 5 ml) and dried under vacuum for elemental analysis. Yellow crystals of **3** suitable for a crystal-structure determination were isolated after recrystallization from CH_2Cl_2/pentane 1:3 at −20°. M.p. 233° (dec.). ^{1}H-NMR (CD_2Cl_2)[1]): 8.31 (*dm*, ^3J = 9.0, 2 H−C(5)); 8.01 (*dm*, ^3J = 7.5, 2 H−C(8)); 7.71 (*tm*, ^3J = 7.5, 2 H−C(6)); 7.59 (*tm*, ^3J = 7.5, 2 H−C(7)); 6.03 (*d*, ^2J = 18.0, H_e−C(10)); 5.57 (*d*, ^2J = 18.0, H_a−C(10)); 4.63 (*m*, 4 H, HC=CH(cod)); 2.69 (*m*, 4 H_{eq}(cod)); 2.05 (*m*, 4 H_{ax}(cod)). ^{13}C{^{1}H}-NMR (CD_2Cl_2)[1]): 165.72 (*s*, C(2)); 150.55 (*s*, C(4)); 134.52 (*s*, C(9)); 128.69 (*s*, C(6)); 128.02 (*s*, C(7)); 124.02 (*s*, C(8)); 121.95 (*s*, C(5)); 85.25 (*d*, J(Rh,C) = 12.07, olef. C); 37.91 (*s*, C(10)); 30.81 (*s*, aliph. C). MS: 493 (71, M^+), 386 (17, [M − cod]$^+$). Anal. calc. for $C_{23}H_{22}BF_4N_2RhS_2$: C 47.6, H 3.8, N 4.8; found: C 47.8, H 3.9, N 4.5.

[Rh(bbte)(cod)]BF_4 (**4**). As described for **3**, from [RhCl(cod)]$_2$ (0.110 g, 0.223 mmol), $AgBF_4$ (0.087 g, 0.447 mmol), and bbte (0.132 g, 0.445 mmol). A light yellow precipitate (0.215 g, 81%) was isolated and dried under vacuum. Crystallization from CH_2Cl_2/pentane 1:3 afforded yellow crystals suitable for a crystal-structure determination. M.p. 136° (dec.). ^{1}H-NMR (CD_2Cl_2)[1]): 8.75 (*dm*, ^3J = 9.0, 2 H−C(5)); 7.85 (*dm*, ^3J = 9.0, 2 H−C(8)); 7.70 (*tm*, ^3J = 7.5, 2 H−C(6)); 7.49 (*tm*, ^3J = 8.25, 2 H−C(7)); 5.40 (*m*, H_e−C(10), H_e−C(10′)); 4.18 (*m*, H_a−C(10), H_a−C(10′)); 4.69 (*s*, H−C(12), H−C(12′) (cod)); 4.48 (*s*, H−C(13), H−C(13′) (cod)); 2.92 (*m*, H_e−C(11), H_e−C(11′) (cod)); 2.74 (*m*, H_e−C(14), H_e−C(14′) (cod)); 2.14 (*m*, 4 H_{ax}(cod)). ^{13}C{^{1}H}-NMR (CD_2Cl_2)[1]): 177.61 (*s*, C(2)); 150.53 (*s*, C(4)); 133.75 (*s*, C(9)); 128.64 (*s*, C(6)); 127.63 (*s*, C(7)); 123.55 (*s*, C(8)); 122.73 (*s*, C(5)); 87.33 (*d*, J(Rh,C) = 11.7, C(12), C(12′)); 83.86 (*d*, J(Rh,C) = 11.7, C(13), C(13′)); 31.17 (*s*, C(10)); 31.09 (*s*, C(11), C(11′)); 30.80 (*s*, C(14), C(14′)). MS: 507 (100, M^+), 399 (12, [M − cod]$^+$). Anal. calc. for $C_{24}H_{24}BF_4N_2RhS_2$: C 48.5, H 4.1, N 4.7; found: C 48.8, H 4.2, N 4.6.

[Rh(CO)$_2$(Hbbtm)]BF_4 (**5**). Carbon monoxide was bubbled through a soln. of **3** (0.101 g, 0.174 mmol) in CH_2Cl_2 (25 ml) for 15 min. The CH_2Cl_2 volume was reduced to 1–2 ml *in vacuo*, after which Et_2O (15 ml) was added to precipitate **5**. The light yellow precipitate (0.069 g, 75%) was isolated by filtration, washed with Et_2O, and dried under vacuum. M.p. 135° (dec.). IR (CH_2Cl_2): 2103.9*s*, 2044.1*s*. IR (nujol): 2095.3*s*, 2027.0*s*. ^{1}H-NMR (CD_2Cl_2)[1]): 8.38 (*dm*, ^3J = 8.6, 2 H−C(5)); 8.10 (*dm*, ^3J = 8.3, 2 H−C(8)); 7.83 (*tm*, ^3J = 7.8, 2 H−C(6)); 7.71 (*tm*, ^3J = 7.7, 2 H−C(7)); 5.66 (*d*, ^2J = 16.7, H_e−C(10)); 5.29 (*d*, ^2J = 16.7, H_a−C(10)). ^{13}C{^{1}H}-NMR (CD_2Cl_2)[1]):

182.73 (*d*, *J*(Rh,C) = 70.1, CO); 168.89 (*s*, C(2)); 150.62 (*s*, C(4)); 133.63 (*s*, C(9)); 129.52 (*s*, C(6)); 128.75 (*s*, C(7)); 124.03 (*s*, C(8)); 122.01 (*s*, C(5)); 36.49 (*s*, C(10)). MS: 441 (45, M^+), 412 (12, $[M-CO]^+$), 385 (31, $[M-2CO]^+$), 282 (17, Hbbtm). Anal. calc. for $C_{17}H_{10}BF_4N_2O_2RhS_2$: C 38.7, H 1.9, N 5.3; found: C 38.6, H 1.8, N 5.4.

[Rh(bbte)(CO)$_2$]BF$_4$ (**6**). As described for **5**, from **4** (0.100 g, 0.168 mmol). A light yellow precipitate (0.077 g, 85%) was isolated. Crystallization from CH_2Cl_2/pentane 1:3 afforded yellow crystals suitable for crystal-structure determination. M.p. 108–112° (dec.). IR (CH_2Cl_2): 2107.0*s*, 2047.6*s*. IR (nujol): 2100.6*s*, 2034.8*s*. ^{1}H-NMR (CD_2Cl_2)^1): 8.56 (*dm*, ^3J = 9.0, 2 H–C(5)); 7.95 (*dm*, ^3J = 9.0, 2 H–C(8)); 7.74 (*tm*, ^3J = 7.5, 2 H–C(6)); 7.59 (*tm*, ^3J = 7.5, 2 H–C(7)); 4.70 (*m*, H_e–C(10), H_e–C(10′)); 4.10 (*m*, H_a–C(10), H_a–C(10′)). ^{13}C{^{1}H}-NMR (CD_2Cl_2)^1). 181.99 (*d*, *J*(Rh,C) = 69.38, CO); 176.03 (*s*, C(2)); 150.45 (*s*, C(4)); 132.80 (*s*, C(9)); 128.94 (*s*, C(6)); 127.95 (*s*, C(7)); 123.33 (*s*, C(8)); 122.36 (*s*, C(5)); 30.68 (*s*, C(10)). MS: 455 (100, M^+), 427 (20, $[M-CO]^+$), 399 (46, $[M-2CO]^+$). Anal. calc. for $C_{18}H_{12}BF_4N_2O_2RhS_2$: C 39.9, H 2.2, N 5.2; found: C 39.9, H 2.4, N 5.3.

[Rh(bbtm)(cod)] (**7**). The ligand Hbbtm (0.234 g, 0.829 mmol) was deprotonated with 1.4M BuLi (0.59 ml, 0.829 mmol) at r.t. in Et_2O. This soln. was slowly added to a soln. of $[RhCl(cod)]_2$ (0.204 g, 0.414 mmol) dissolved in Et_2O, and the mixture turned red immediately. The volatiles were evaporated. The precipitate was washed with Et_2O (2 ml) and dried under vacuum: **7** (0.246 g, 60%). Orange-red powder. ^{1}H-NMR (CD_2Cl_2)^1): 7.65 (*dm*, ^3J = 6.0, 2 H–C(5)); 7.43 (*dm*, ^3J = 6.0, 2 H–C(8)); 7.20 (*tm*, ^3J = 7.5, 2 H–C(6)); 6.96 (*tm*, ^3J = 6.0, 2 H–C(7)); 5.41 (*s*, H–C(10)); 4.19 (*m*, 4 H, HC=CH (cod)); 2.40 (*m*, 4 H_{eq} (cod)); 1.64 (*m*, 4 H_{ax} (cod)). ^{13}C{^{1}H}-NMR (CD_2Cl_2)^1): 163.44 (*s*, C(2)); 152.32 (*s*, C(4)); 131.22 (*s*, C(9)); 125.68 (*s*, C(6)); 121.81 (*s*, C(7)); 121.14 (*s*, C(8)); 117.96 (*s*, C(5)); 85.14 (*s*, C(10)); 78.14 (*d*, *J*(Rh,C) = 13.58, olef. C(cod)); 30.55 (*s*, aliph. C (cod)). FAB-MS: 493 (73, M^+), 385 (4, $[M-cod]^+$). Anal. calc. for $C_{23}H_{21}N_2RhS_2$: C 56.1, H 4.3, N 5.7; found: C 56.3, H 4.4, N 5.5.

[Rh(bbtm)(CO)$_2$] (**8**). As described for **5**, with **7** (0.148 g, 0.300 mmol) (on CO_2 bubbling, red → orange; precipitation with cold Et_2O). The orange precipitate (0.085 g, mmol, 64%) was isolated immediately by filtration, washed with cold Et_2O (2 ml), and dried under vacuum. IR (CH_2Cl_2): 2074.6*s*, 2007*s*. ^{1}H-NMR (CD_2Cl_2)^1): 7.79 (*dm*, ^3J = 6.0, 2 H–C(5)); 7.57 (*dm*, ^3J = 6.0, 2 H–C(8)); 7.40 (*tm*, ^3J = 6.0, 2 H–C(6)); 7.18 (*tm*, ^3J = 9.0, 2 H–C(7)); 5.78 (*s*, H–C(10)). ^{13}C{^{1}H}-NMR (CD_2Cl_2)^1): 187.75 (*d*, *J*(Rh,C) = 67.9, CO); 162.65 (*s*, C(2)); 153.84 (*s*, C(4)); 129.30 (*s*, C(9)); 126.61 (*s*, C(6)); 123.30 (*s*, C(7)); 121.51 (*s*, C(8)); 119.87 (*s*, C(5)); 83.84 (*s*, C(10)). FAB-MS: 441 (19, M^+), 413 (4, $[M-CO]^+$), 385 (6, $[M-2CO]^+$). Anal. calc. for $C_{17}H_9N_2O_2RhS_2$: C 46.37, H 2.06, N 6.36; found: C 46.2, H 2.0, N 6.4.

Crystal-Structure Determinations. The diffraction data were collected on a *Nonius-Kappa-CCD* diffractometer with graphite-monochromated Mo-K_α radiation (λ 0.71073 Å), with ϕ and ω scans to fill the *Ewald* sphere (*Nonius* COLLECT [25]). Data reduction was performed with DENZO [26]. The initial structure solution was found by direct methods, while the rest of the atomic positions were found from difference *Fourier* maps. All non-H-atoms were refined anisotropically by full-matrix least-squares methods. The H-atoms were fixed in calculated positions. All calculations were performed with SHELX-97 [27] within the WINGX package [28]. Figures were generated with Ortep3 for Windows [29]; displacement ellipsoids are at the 50% probability level.

Crystal Structure of **3**. Diffraction data were collected at 173(2) K. Formula. $C_{23}H_{22}BF_4N_2RhS_2$, M_r 580.27; yellow prismatic crystal, crystal size 0.25 × 0.11 × 0.07 mm; unit-cell parameters: a = 11.1969(2), b = 14.1646(3), c = 14.4392(3) Å, $\alpha=\beta=\gamma=90°$; crystal system orthorhombic; space group $P2_12_12_1$; V = 2290.05(8) Å^3; F(000) = 1168; formula units Z = 4, calc. density 1.683 g cm^{-3}; linear absorption coefficient 0.975 (μ/cm^{-1}). Of 12206 reflections measured, 4467 reflections were unique; 318 parameters were refined. The θ-range for data collection was 2.01–26.00° with indices hkl −11 to 14, −18 to 16, and −18 to 12. The final indices were R = 0.0284; wR = 0.0448 and R = 0.0362, wR = 0.0468 (final data) with a goodness-of-fit 1.000. The largest difference peak and hole were 0.402 and −0.405 eÅ^{-3}.

Crystal Structure of **4**. Diffraction data were collected at 173(2) K. Formula $C_{25}H_{26}BClF_4N_2RhS_2$, M_r 679.20; yellow prismatic crystal, crystal size 0.24 × 0.20 × 0.15 mm; unit-cell parameters: a = 22.4448(2), b = 21.4709(2), c = 13.51640(10) Å, α = 90, β = 126.5750(10), γ = 90°; crystal system monoclinic; space group $C2/c$; V = 5230.99(10) Å^3; F(000) = 2720; formula units Z = 4, calc. density 1.720 g cm^{-3}; linear absorption coefficient 1.065 (μ/cm^{-1}). Of 18406 reflections measured, 5147 reflections were unique; 347 parameters were refined. The θ-range for data collection was 1.48–26.00° with indices hkl −27 to 27, −28 to 26, and −16 to 14. The final indices were R = 0.0218, wR = 0.0500 and R = 0.0268, wR = 0.0540 (final data) with a goodness-of-fit 1.071. The largest difference peak and hole were 0.524 and −0.426 e Å^{-3}.

Crystal Structure of **6**. Diffraction data were collected at 173(2) K. Formula $C_{19}H_{14}BCl_2F_4N_2O_2RhS_2$, M_r 627.06; yellow prismatic crystal, crystal size $0.21 \times 0.17 \times 0.15$ mm; unit-cell parameters: $a = 14.0586(2)$, $b = 21.7941(3)$, $c = 15.1994(3)$ Å, $\alpha = 90$, $\beta = 102.6380(10)$, $\gamma = 90°$; crystal system monoclinic; space group $C2/c$; $V = 4544.18(13)$ Å^3; $F(000) = 2480$; formula units $Z = 8$, calc. density 1.833 g cm^{-3}; linear absorption coefficient 1.224 (μ/cm^{-1}). Of 13478 reflections measured, 4957 reflections were unique; 299 parameters were refined. The θ-range for data collection was 1.75–27.00° with indices hkl −17 to 17, −27 to 25, and −19 to 19. The final indices were $R = 0.0304$, $wR = 0.0730$ and $R = 0.0399$, $wR = 0.0782$ (final data) with a goodness-of-fit 1.079. The largest difference peak and hole were 0.547 and −0.796 e Å^{-3}.

Crystallographic data for the structures in this paper have been deposited with the *Cambridge Crystallographic Data Centre (CCDC)* as supplementary publication no. 187098 (**3**), 187099 (**4**), and 187100 (**6**). Copies of the data can be obtained, free of charge, on application to CCDC, 12 Union Road, Cambridge CB21EZ, UK (fax: +441223336033; e-mail: deposit@ccdc.cam.ac.uk).

We thank *Johnson Matthey*, PLC for the generous loan of $RhCl_3$.

REFERENCES

[1] M. Marchetti, G. Mangano, S. Paganelli, C. Botteghi, *Tetrahedron Lett*. **2000**, *41*, 3717.
[2] S. Elgafi, L. D. Field, B. A. Messerle, P. Turner, T. W. Hambley, *J. Organomet. Chem*. **1999**, *588*, 69.
[3] S. Burling, L. D. Field, B. A. Messerle, *Organometallics* **2000**, *19*, 87.
[4] S. Elgafi, L. D. Field, B. A. Messerle, *J. Organomet. Chem*. **2000**, *607*, 97.
[5] F. Ragaini, M. Pizzotti, S. Cenini, A. Abbotto, G. A. Pagani, F. Demartin, *J. Organomet. Chem*. **1995**, *489*, 107.
[6] L. A. Oro, M. Esteban, R. M. Claramunt, J. Elguero, C. Foces-Foces, F. H. Cano, *J. Organomet. Chem*. **1984**, *276*, 79.
[7] P. Kalck, A. Thorez, M. T. Pinillos, L. A. Oro, *J. Mol. Catal.* **1985**, *31*, 311.
[8] R. Uson, L. A. Oro, M. T. Pinillos, *J. Mol. Catal*. **1982**, *14*, 375.
[9] M. D. Fryzuk, L. Jafarpour, S. J. Rettig, *Tetrahedron: Asymmetry* **1998**, *9*, 3191.
[10] G. Esquius, J. Pons, R. Yăñez, J. Ros, *J. Organomet. Chem*. **2001**, *619*, 14.
[11] H. Schumann, H. Hemling, V. Ravindar, Y. Badrieh, J. Blum, *J. Organomet. Chem*. **1994**, *469*, 213.
[12] C. B. Dieleman, P. C. J. Kamer, J. N. H. Reek, P. W. N. M. van Leeuwen, *Helv. Chim. Acta* **2001**, *84*, 3269.
[13] M. Polievka, A. Jegorov, L. Uhlár, V. Macho, *Collect. Czech. Chem. Commun.* **1984**, *46*, 1677.
[14] L. A. Oro, M. A. Ciriano, F. Viguri, *Inorg. Chim. Acta* **1986**, *115*, 65.
[15] M. Witanowski, W. Sicinska, Z. Biedrzycka, Z. Grabowski, G. A. Webb, *J. Chem. Soc., Perkin Trans. 2* **1996**, 619.
[16] R. F. Fenske, in 'Organometallic Compounds, Synthesis, Structures and Theory', Ed. B. L. Shapiro, Texas A & M University Press, Texas, 1983, p. 305.
[17] D. L. Pavia, G. M. Lampman, G. S. Kriz, 'Introduction to Spectroscopy, A Guide for Students of Organic Chemistry', 2nd edn., Saunders College Publishing, Fort Worth, 1996, p. 220.
[18] W. A. Herrmann, M. Elison, J. Fischer, C. Köcher, G. R. J. Artus, *Chem.–Eur. J.* **1996**, *2*, 772.
[19] H. G. Raubenheimer, E. K. Marais, S. Cronje, C. Esterhuysen (neé Thompson), G. J. Kruger, *J. Chem. Soc., Dalton Trans.* **2000**, 3016.
[20] M. T. Ramos, C. Avendano, C. Elguero, F. Florencio, J. Sanz-Aparicio, *Inorg. Chim. Acta* **1990**, *174*, 169.
[21] R. J. Errington, 'Advanced Practical Inorganic and Metalorganic Chemistry', Chapman & Hall, London, 1997, p. 92.
[22] M. R. Winkle, J. M. Lansinger, R. C. Ronald, *J. Chem. Soc., Chem. Commun*. **1980**, 87.
[23] C. Rai, J. B. Braunwarth, *J. Org. Chem*. **1961**, *25*, 3434.
[24] W. A. Herrmann, C. Zybril, in 'Synthetic Methods of Organometallic and Inorganic Chemistry', Eds. W. A. Herrmann and A. Salzer, Georg Thieme Verlag, Stuttgart, 1996, Vol. 1, p. 150.
[25] COLLECT, Data Collection Software, Nonius BV, Delft, The Netherlands, 1998.
[26] Z. Otwinowski, W. Minor, *Methods Enzymol*. **1997**, *276*, 307.
[27] G. M. Sheldrick, 'SHELX-97, Program for Crystal Structure Analysis', University of Göttingen, Germany, 1997.
[28] L. J. Farrugia, *J. Appl. Crystallogr.* **1999**, *32*, 837.
[29] L. J. Farrugia, *J. Appl. Crystallogr.* **1997**, *30*, 565.

Received June 12, 2002